Study of Globular Clusters

A thesis submitted in partial fulfillment of the requirement
for the degree of Bachelor of Science in
Physics from the College of William and Mary in Virginia,

by

Lena Sherbakov.

Advisor: Dr. Carl Carlson.

Williamsburg, Virginia
May 2005

Abstract

In the study of globular clusters, the King distribution function has been the standard for modeling the velocity dispersion, luminosity and surface density profiles. However, based on star count analysis developed by Grillmair *et al.* [5], it is apparent that there exist stars outside of the King tidal radius (while the model predicts that stars should no longer be bound to the globular cluster). Moreover, the star counts depart from the King model even at radii considerably less than the tidal radius. In this paper, we use the star count data developed by Grillmair *et al.* [5] and fit them to a Michie model (an extension of the King model that considers an extra parameter: the anisotropic radius of the cluster). Our results show that the Michie distribution function is more accurate than the more popular King distribution function. This result validates the belief that the velocity dispersions of stars in a globular cluster are not isotropic at all radii. Furthermore, I will consider the possibility that the deviation in star counts from the King model is attributed to the presence of dark matter. However, our results imply that adding dark matter to a Michie model does not improve the fit, largely because the model does not permit the dark matter to extend beyond the tidal radius. Due to this limitation in the models, no statements about the amount of dark matter in a globular cluster can be made.

Acknowledgements

I would like to thank Dr. Carl Carlson for his help as my advisor.

Contents

1 Introduction

In this thesis, we study the space and velocity distribution of stars in a globular cluster. The goals are to determine, by fitting the observed distribution profiles, whether anisotropy in the velocity distribution is necessary to describe the observations, and to find limits on the amount of dark matter that may be concentrated within a globular cluster.

Two useful generic forms for the distribution functions were given by I.R. King [9] and by R. Michie [10]. In order to understand the distribution functions developed by King and Michie, it is essential to review the general dynamics of globular clusters. In the Overview (section 1.1), I will give a brief explanation of how stars escape the cluster, followed by some simple calculations of the characteristic size, mass, density, and visible luminosity of a typical globular cluster (here the term *typical* is used rather loosely since globular clusters tend to vary quite a bit.)

However, to find an effective model that fits the surface density data for globular clusters proves to be a difficult task. Both the King and Michie models relate the number distribution or mass distribution of stars at a given point to the potential at that point. The potential, in turn, is given in terms of the density by Poisson's equation. Hence one knows neither the potential nor the stellar distribution until one has solved Poisson's equation self-consistently. The description of how this is done, and results for selected globular cluster are in Section 3 of this paper.

Depending on the level of accuracy sought, one needs not only an accurate generic model to describe the cluster, one must also consider and pick the right values for the many parameters involved. Some of these parameters include the radius of anisotropy, the tidal radius, and the dark to light matter ratio. Since the globular cluster sits in the (non-uniform) gravitational field of its parent galaxy, there is a tidal radius, r_t, beyond which tidal forces from the galaxy will pull stars loose from the cluster. The anisotropy radius will be defined later in this paper.

Throughout this paper, I will use the modified star count profiles developed by Grillmair *et al.* [5]. The problem with raw star counts at $r \approx r_t$ (tidal radius), is the difficulty in differentiating between background and foreground stars from those that belong to the globular cluster. In addition, the problem with raw star counts for $r \ll r_t$ is that they do not account for crowding effects. However, Grillmair *et al.* [5] has already compensated for these two complications in his adjusted star count data for twelve globular clusters.

The data from Grillmair *et al.* [5] has led to the unmistakable observation that there is a clear discrepancy between the star count profiles and the King models at radii near r_t. King models are the only models that Grillmair *et al.* considered. The fact that there are stars outside of the tidal radius (tidal tails) is somewhat understandable since it has already been shown that the removal of loosely-bound cluster stars by tidal forces of the Galaxy is for some stars a slow process; clusters may be surrounded by halos of unbound stars for many Galactic orbits [7].

However, an even more interesting observation made by Grillmair *et al.* [5] is that in all 12 clusters observed, the star counts depart from the King models at radii considerably less than r_t. Moreover, there are more stars than anticipated in this outer part of the cluster, which is still inside the tidal radius. Granted that some of these extra stars may still be background stars, Grillmair also believes that the error may lie in King values for the tidal radii. It is possible that r_t is smaller than King's r_t (in which case these stars that deviate from the King model inside the tidal radius, appropriately nicknamed extra tidal stars, also become tidally removed.) Alternatively, Grillmair suggests that the tidal radius may be much larger than King's r_t. This hypothesis arises from the observation that the extra tidal stars are nicely fitted by power laws. Thus, if one fits the extension and the main body of the surface density profile of a globular cluster simultaneously, the King radius is much smaller than the actual tidal radius [5].

However, an appropriate alternative to the King model that Grillmair does not consider is the Michie model. Since the Michie model has an extra parameter (radius of anisotropy), it is more flexible to fit the observed data. A large portion of this paper is dedicated to exploring the benefits of this model.

Another explanation for the presence of stars outside of the tidal radius is the existence of a dark matter halo surrounding the globular cluster that keeps these stars bound to the cluster. Grillmair *et al.* does not consider this alternative, although it is possible to develop a two-component surface density model that accounts for the mass segregation. The last section of this paper is devoted to developing and analysing such a two-component model. The last possibility to consider is that the star count observations deviate from the King model due to a different law of gravity dominating in globular clusters at distances $r \approx r_t$. The last possibility is interesting to consider but is beyond the scope of this paper.

1.1 Overview

To understand how globular clusters behave, we first consider the most basic approach and determine how well it coincides with our observations. In this simplistic simulation, the masses of all the stars are assumed to be identical and tidal forces acting on the globular cluster have been neglected. The globular cluster is assumed to be statistically steady, spherical, and self-gravitating. Moreover, the velocity distribution of the stars is assumed to be isotropic (same velocity in all directions). Thus, under these conditions we use the virial theorem to relate the total kinetic energy of a globular cluster with N stars of mass m to the total gravitational potential energy [1]:

$$\frac{Nmv^2}{2} = \frac{GN(N-1)m^2}{4R}. \tag{1}$$

Here R refers to the core radius and v is the root mean square velocity of stars. Typically there are three radii when discussing globular clusters: the first is the core radius r_c (radius at which surface brightness diminishes to half the central value), the

second is the half light radius r_h (radius that contains half of the light of the cluster or half of the visible mass of the cluster), and the third is the tidal radius r_t beyond which the external gravitational field of the galaxy dominates the dynamics [4].

To determine the escape velocity from Eq. (1), we compare the kinetic energy of the mass that is trying to escape to the potential energy between that one star of mass m and the rest of the globular cluster of mass M. From this simple calculation, it can be shown that the escape velocity is twice v_{rms} for the globular cluster. Moreover, the distribution of stellar velocities is entirely analogous to the thermodynamic distribution of random velocities in a classical gas; most stars have this dispersive speed v_{rms} and the velocity dispersion itself can be fit to a Maxwell-Boltzmann distribution. Through collisions, there is a tail of stars that attain speeds greater than v_{rms} and escape the cluster. Once this occurs, we must compute the time it takes for the entire cluster to readjust its v_{rms} and repeat this process over again. The time it takes a globular cluster to readjust its random velocity distribution is called the relaxation time. Creating a reasonable model for the relaxation time of a globular cluster involves analyzing how small deflections affect the typical random velocity of stars. The relaxation time is agreed upon in most books to be governed by the equation [1]:

$$t_{relax} = \left(\frac{r_c}{v_{rms}}\right) \frac{N}{12ln(N/2)}. \tag{2}$$

I will often write $\frac{r_c}{v_{rms}}$ as the crossing time t_{cross}. From this relaxation model, to find the time that it takes for all the stars in the cluster to escape, we simply look at the tail ends of this Maxwellian distribution. The fraction ξ of stars that will escape in one relaxation time is just the fraction of stars that are in that tail end of the distribution (those stars that have reached velocities that exceed twice the root mean square velocity. I will call this fraction of stars $P_M(v)$). Thus, ξ is given by [2]:

$$\xi = \int_{2v_{rms}}^{\infty} P_M(v)dv = 7.4 \times 10^{-3}. \tag{3}$$

Since we can divide out this fraction of stars after each relaxation time (because they are no longer a part of the cluster), the evaporation time is given by,

$$t_{evap} = \frac{t_{relax}}{\xi} \approx 135 t_{relax} \tag{4}$$

However, as Spitzer pointed out, detailed mechanics of the escape of stars from the cluster depend on the ratio of relaxation time to the crossing time, and thus depend on the number of stars in the globular cluster. Typically, for a globular cluster containing 10^6 stars, the evaporation time is closer to $t_{evap} = 100 t_{relax}$ [2].

This basic model of the dynamics of globular clusters helps us evaluate more complicated models involving tidal forces, anisotropic velocity dispersions, and the addition of dark matter in the mass distribution function. In the following sections, using standard values for the mass, density, number of stars, and radius of a globular cluster, I will show the results of several elementary calculations for the evaporation times, minimum radii based on star counts, and acceleration of stars near the escape radius. I will then consider more involved models such as the King and Michie distributions of the number of stars per unit volume in coordinate space per unit volume in volume space.

2 Elementary Calculations

Before proceeding with more complicated calculations, we need to develop an understanding for the basic properties of a globular cluster (assuming it abides by the model in the overview.) Such properties are the number of stars, the average mass of a star, the visible central density, total visible luminosity, v_{rms}, and various radii. Table 1 sums up these observables and deduced values (notice that there are some discrepancies between different sources). From this data, the evaporation time of a globular cluster is approximated by Eqs. (2) and (4) to be 80 billion years (much greater than the projected age of the universe). An interesting calculation is to see

Table 1: Values for a Typical Globular Cluster

# of stars [1]	avg. mass of star [1]	vis. central density [6]	total vis. luminosity [6]
10^6	$.5M_\odot$	$8000M_\odot/pc^3$	$3 \times 10^5 L_\odot$
v_{rms} [1], [6]	r_c [1], [4]	r_h [4]	r_t [4]
$20km/s, 7km/s$	$8.3 \times 10^{16}m, 4.63 \times 10^{16}m$	$3.09 \times 10^{17}m$	$1.5 \times 10^{18}m$

what the minimum radius of a globular cluster should be in order for it to still be around today. In other words, set t_{evap} to be the age of the universe (15 billion years) and rearrange the equations to find the minimum radius of that cluster. For a globular cluster consisting of 10^6 stars, the minimum radius is $3.42 \times 10^{16}m$, which is smaller than the radius of any measured globular cluster that exists today.

As discussed in the introduction, globular cluster may also have a two-component distribution function. In an attempt to calculate the amount of dark matter that could be present, the question arises: why is it not possible to tag a star that lies just outside of the escape radius of a globular cluster (presumably gone from the cluster based on our model), figure out its velocity (using red shifts and blue shifts), measure the velocity of the same star after one year, and see whether it is accelerating or decelerating. If the star is accelerating, it is gone from the cluster like our model predicted; however, if the star is decelerating, it is being pulled back by the cluster because the cluster is more massive than just the visible matter. As it turns out, the change in velocity of the star in one year, or even a few years is too small to determine whether it is accelerating or decelerating. The change in velocity of a globular cluster at the escape radius (or tidal radius) is $9.3 \times 10^{-4}m/s$ in one year.

Using this simple model, we have determined ballpark figures for minimum radii, escape velocities and accelerations of stars in the globular clusters. Now we can look at more realistic models that take into consideration the tidal forces and non-isotropic velocity dispersions.

3 King and Michie Models

3.1 King Model Density Profiles

A globular cluster experiences a tidal force due to the galactic center. Once a star that is part of a globular cluster reaches a tidal radius, the external gravitational field of the galaxy dominates its dynamics and it is no longer bound to the cluster. Moreover, these values for the tidal radius have previously been worked out by King and alterations have been suggested by Grillmair *et al.* [5].

A well known model that accounts for the existence of a tidal forces and predicts the distribution of stars in a cluster to a reasonable degree of accuracy is the King model. This model assumes that the velocity distribution is isotropic everywhere (same in all directions). The King model for the phase space distribution of a stellar species is the following:

$$f(r,v) = \begin{cases} 0, & \epsilon < 0 \\ k\left(e^{2j^2\epsilon} - 1\right), & \epsilon > 0, \end{cases} \tag{5}$$

where $\epsilon = V(r_t) - (V(r) + v^2/2)$, and $V(r_t)$ is the gravitational potential at the tidal radius. Here j is inversely proportional to the velocity dispersion. That is to say, $j = \frac{1}{\sqrt{2}\sigma}$, where σ is some constant. The constant k is the normalization factor and can, as an alternative, be replaced by the central density. Notice that this distribution represents a Maxwellian. We set zero potential to be at the boundary of the cluster defined by the tidal radius r_t; in other words, $V(r_t) = 0$. The escape velocity at any point is given by ${v_e}^2 = -2V(r)$. Thus when the expression $V(r)+v^2/2$ is positive, implying ϵ is negative and the star has escaped (or will escape) the cluster, the distribution function disappears. However, when ϵ is positive, the velocities are spherically distributed.

As King had done earlier [8], we are interested in obtaining an expression for the surface density of a globular cluster. This is defined as the number of stars per unit volume in coordinate space per unit volume in volume space. By substituting in the expression for ϵ, and multiplying by 1 ($e^{-2j^2V(r)}e^{2j^2V(r)}$), we can rewrite Eq. (5) as:

$$f(r,v) = ke^{-2j^2V(r)}(e^{-j^2v^2} - e^{2j^2V(r)}). \tag{6}$$

To simplify further, we let $W = -2j^2V(r)$ and $\eta = j^2v^2$. The expression for the density ρ can now be written as:

$$\rho = \int_0^{v_e} f(v,r)4\pi v^2 dv = 2\pi kj^{-3}e^W \int_0^W (e^{-\eta} - e^{-W})\eta^{\frac{1}{2}} d\eta. \tag{7}$$

Similarly ρ_0, the central density, is defined as:

$$\rho_0 = 2\pi kj^{-3}e^{W_0} \int_0^{W_0} (e^{-\eta} - e^{-W})\eta^{\frac{1}{2}} d\eta, \tag{8}$$

where $W_0 = W(0)$. We can perform one integration by parts to simplify ρ and ρ_0 to:

$$\rho = \frac{4}{3}\pi kj^{-3}e^W \int_0^W e^{-\eta}\eta^{\frac{3}{2}} d\eta. \tag{9}$$

$$\rho_0 = \frac{4}{3}\pi kj^{-3}e^{W_0} \int_0^{W_0} e^{-\eta}\eta^{\frac{3}{2}} d\eta. \tag{10}$$

The last integrals were done with the help of Mathematica 5.0, to yield:

$$\rho/\rho_0 = 0.2374e^{W(r)}(\frac{3}{4}\sqrt{\pi}\mathrm{Erf}[\sqrt{W(r)}] - \frac{1}{2}e^{-W(r)}\sqrt{W(r)}(3 + 2W(r))). \tag{11}$$

At this point, we have an expression for density in terms of $W(r)$, but what we wish to have is an expression $\rho(r)$. This can be done by solving Poisson's equation using W in place of the potential V, and the dimensionless radius $R = r/r_c$, where r_c is a scale factor still called the core radius. Poisson's equation now reads:

$$\frac{d^2W}{dR^2} + \frac{2}{R}\frac{dW}{dR} = -8\pi Gj^2{r_c}^2\rho. \tag{12}$$

Based on King's earlier works [9], the core radius is chosen so that the central value of $\nabla^2 W$ is -9 (so as to be in agreement with an earlier different definition of the core

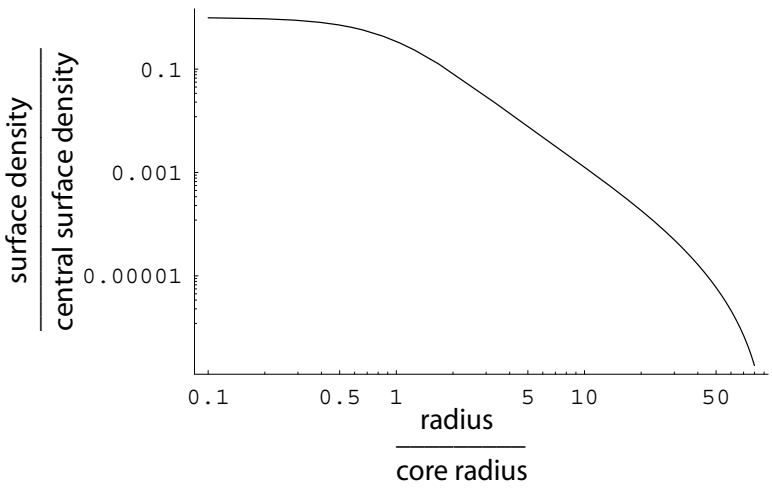

Figure 1: ρ/ρ_0 vs. R ($R_t = 100$)

radius cited in the Overview). We write $8\pi G j^2 {r_c}^2 \rho_0 = 9$, and now Eq. (12) reads [8]:

$$\frac{d^2W}{dR^2} + \frac{2}{R}\frac{dW}{dR} = -9\frac{\rho}{\rho_0}. \tag{13}$$

To solve this differential equation, we used the NDSolve tool in Mathematica 5.0, which gave a result for $W(R)$ in terms of an interpolating function. Substituting this interpolating function for $W(R)$, we now have a density function ρ/ρ_0. However, if we want to obtain density values for a specific tidal radius, we must know what the corresponding W_0 is. To find this W_0 corresponding to a desired R_t, we input an arbitrary W_0 into Eqs. (10) and (13), and then calculated the resulting value $W(R_t)$ from Eq. (13). We narrowed in on our W_0 with this guess and check method; when our value for $W(R_t)$ was close enough to zero ($\pm$ .001), we had found our W_0. Figure 1 is a LogLogPlot created by Mathematica for $R_t = 100$ ($W_0 = 8.57$) of ρ/ρ_0 vs. R. Although we have constructed an appropriate function ρ/ρ_0, to be able to compare this model to our observations of globular clusters as seen from earth, we need to project ρ/ρ_0 onto the sky. Figure 2 is an illustration of how we would see the cluster from earth; in other words, we have $\rho(R)$, but what we want is $\rho(r)$ (which we later call $\sigma(R)$ to avoid confusion with the non-projected density profile). The new

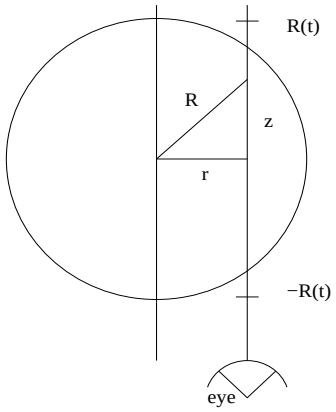

Figure 2: Projection of ρ onto the sky: the globular cluster and our sight line as seen from above.

projected density is now given by the equation:

$$\sigma(r) = \int_{-R_t}^{R_t} \rho(R) dz, \tag{14}$$

where $z = \sqrt{R^2 - r^2}$ (see Figure 2). Also due to symmetry, the bounds of integration can be simplified to $z = 0$ to $z = R_t$ (or $R = r$ to $R = R_t$) - we obviously now need a factor of 2 in front of the integral. The projected density function can be rewritten as follows:

$$\sigma(r) = 2 \int_{r}^{R_t} \frac{R}{\sqrt{R^2 - r^2}} \rho(R) dR, \tag{15}$$

with

$$\sigma_0 = 2 \int_{0}^{R_t} \rho(R) dR. \tag{16}$$

Figure 3 is the resulting LogLogPlot of σ/σ_0 vs. R (where again, R is the dimensionless variable r/r_c). It agrees with similar plots done by King [9]. Now we have the tools to compare observed data to our model. Grillmair *et al.* uses this King model to compare the star count surface density to his observation of 12 globular clusters. They show that the King distribution deviates from the observed data at R slightly less than R_t [5]. A question to consider later in this paper is how would adjusting the model to include dark matter improve or worsen the correlation between the model and the observed data both at $R < R_t$ and $R > R_t$.

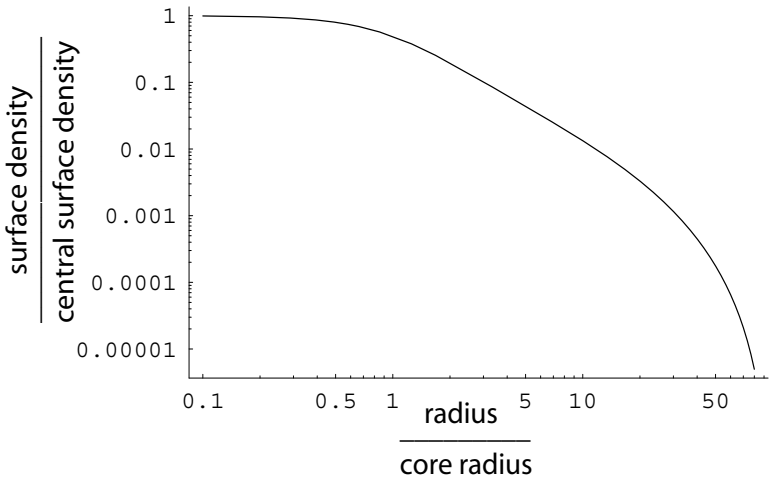

Figure 3: σ/σ_0 vs. R ($R_t = 100$)

3.2 Michie Model Density Profiles

However, before adding dark matter to the King model, we must first consider the Michie model. Although the King model is accurate to some degree, it is possible that the velocity dispersion of stars in a globular cluster change from nearly isotropic at the center to nearly radial (anisotropic) at the scaled radius R_a (radius of anisotropy) [4]. The King model does not account for this anisotropy. The most acclaimed model that takes this fact into consideration is the Michie distribution function. To make the velocity dispersion anisotropic, the Michie distribution in phase space is simply an angular-momentum exponential cut off applied to the King distribution. The following is the Michie distribution function:

$$f(r,v) = \begin{cases} 0, & \epsilon < 0 \\ ke^{-j^2L^2/r_a^2}\left(e^{2j^2\epsilon} - 1\right), & \epsilon > 0, \end{cases} \tag{17}$$

where L is the orbital momentum of the star and is given by $L = rv\sin(\theta)$, and ϵ as before. The constant r_a is the radius of anisotropy. To find the surface density distribution function $\rho(R)$, we mirror the steps we took with the King model. After

substituting in the expression for ϵ and defining W and η in the same manner, our expression for $\rho(W)$ becomes a double integral:

$$\rho = 2\pi kj^{-3}e^{W}\int_0^W d\eta\ (e^{-\eta}-e^{-W})\eta^{\frac{1}{2}}\int_0^{2\pi} d\theta\ \left(e^{\frac{-\eta R^2}{{r_a}^2}}sin^2\right). \tag{18}$$

Letting $y = \cos\theta$, our expressions for ρ and ρ_0 simplify to:

$$\rho = 2\pi kj^{-3}e^{W}\int_0^W d\eta\ (e^{-\eta}-e^{-W})\eta^{\frac{1}{2}}\int_0^{1} dy\ \left(e^{\frac{-\eta R^2}{{r_a}^2}(1-y^2)}\right), \tag{19}$$

and (since L dissappears at $r = 0$)

$$\rho_0 = \frac{4\pi}{3}kj^{-3}e^{W_0}\int_0^{W_0} e^{-\eta}\eta^{3/2}d\eta. \tag{20}$$

These integrals are again done by Mathematica 5.0. Since we already have a relation between W and R (Eq. (13)), we can plot the unprojected ρ/ρ_0 for any desired R_a. To project the ρ/ρ_0 onto the sky, we use exactly the same technique as with the King model. Figures 4 and 5 show the projected density (σ/σ_0) as a function of R (for $R_t = 100$) with $R_a = 100$ and $R_a = 1$ respectively. Notice that at $R_a = 100$, the velocity dispersion is almost entirely isotropic, hence the model mirrors the King model. At $R_a = 1$, notice that the anisotropy makes σ/σ_0 less flat.

Although Grillmair *et al.* [5] has already fitted a King model to his star count data and shown that the observations depart from the model slightly before R_t, there was no attempt to fit the data to a Michie model. In the next section, I will adjust the parameters R_a and R_t in the Michie model in an attempt to better fit the Grillmair *et al.* observed data. After having done this, one may consider fitting a two-component model (one that contains dark matter) to the observed data. However, in the following section I only focus on the following result: adjusting the radius of anisotropy and the tidal radius, the Michie model is a better fit, in particular, to the observed data for two globular clusters that could not be fit well with a King model.

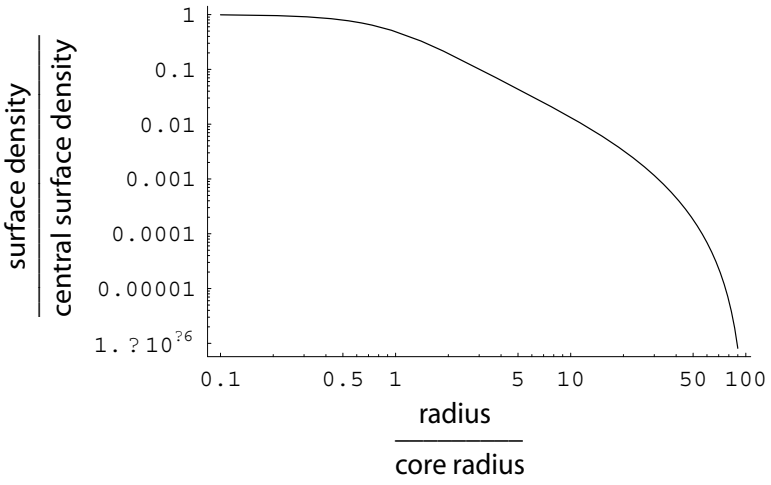

Figure 4: σ/σ_0 vs. R ($R_t = 100$, $R_a = 100$)

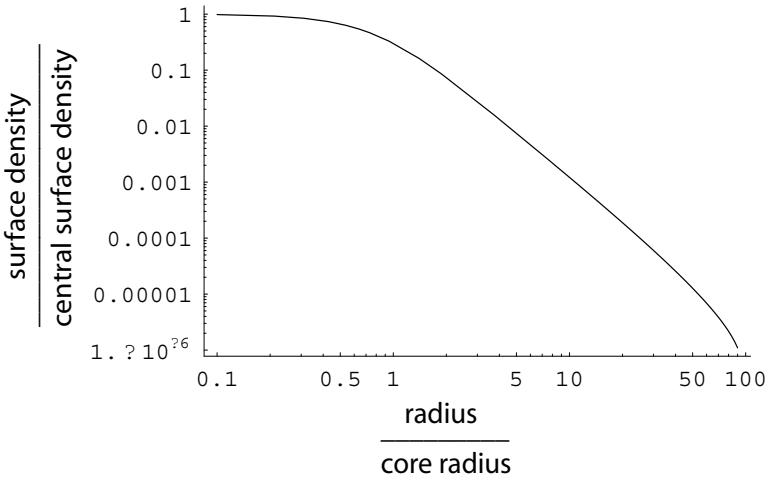

Figure 5: σ/σ_0 vs. R ($R_t = 100$, $R_a = 1$)

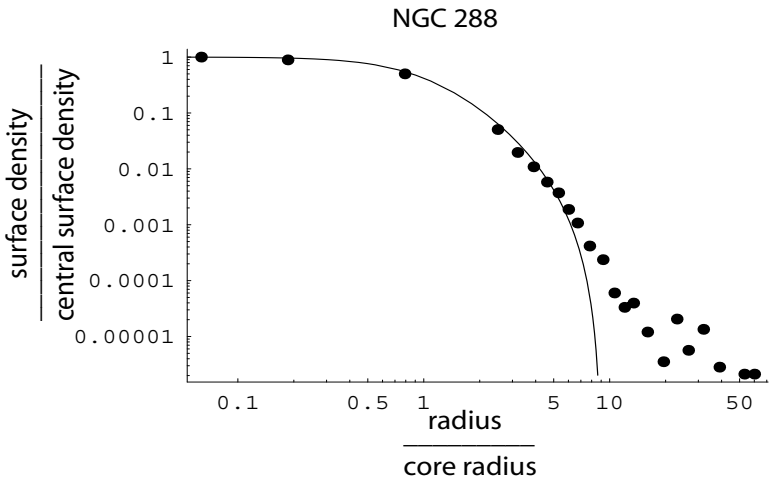

Figure 6: σ/σ_0 vs. R ($R_t = 9.28$)

4 Michie Model Results

Grillmair *et al.* fit the King surface density function to twelve globular clusters [5]. As noted before, for the majority of the globular clusters, the King model is a good fit in the body of the cluster. However, as $r \to r_t$, the star counts start to deviate significantly from the model. In particular, for almost all of these globular clusters, there are a noticeable number of stars that lie outside of the tidal radius, beyond which, no stars should exist. However, pushing out the tidal radius of these globular clusters to include the stars at $r > r_t$ destroys the fit in the body of the cluster. This suggests that the King model is not entirely accurate. The results in this section suggest that the Michie model is a better fit to the globular clusters than the King model used by Grillmair *et al.*.

Out of the twelve globular clusters observed by Grillmair*et al.*, I chose to fit a Michie model to the two that display the worst fit by the King model (NGC 288 and NGC 5824). Figures 6 and 7 show the King model fits to NGC 288 and NGC 5824 respectively. Notice that for NGC 288, the King model fit becomes relatively poor at $R = r/r_c = 7.04$ while the NGC 5824 King model fit is poor throughout the cluster.

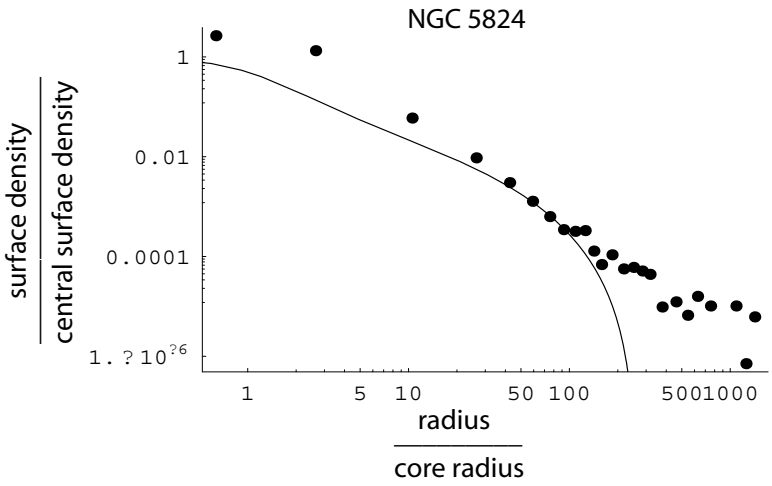

Figure 7: σ/σ_0 vs. R ($R_t = 260$)

In fitting a Michie model to NGC 288, we used the same central density, tidal radius, and core radii as in the Grillmair *et al.* paper ($\sigma_0 = 1412.5$ stars/(armin^2), $r_c = 1.42$ arcmin, $r_t = 12.9$ arcmin) [5]. The data points are also taken from Grillmair's paper (both Grillmair's own data and the data of others that he uses and sites). By adjusting the two parameters in the Michie model (R_a and R_t), we found a better fit to NGC 288 than Grillmair's King model fit; our adjusted values are $R_t = r_t/r_c = 17$, and $R_a = r_a/r_c = 1$. Notice that this Michie model, Figure 8, fits five more points at the edge of the cluster while not disturbing the fit in the body of the cluster. The low value of R_a implies that unlike the King model, the cluster is very anisotropic (only approximately 1/17 of the cluster near the very center has an isotropic velocity dispersion).

Unlike NGC 288, NGC 5824 does not resemble a King distribution at any radius (see Figure 8). Therefore, the fact that our Michie model was able to give a much nicer fit to this globular cluster is a strong result that supports the use of a Michie model over a King model. Similar to how we produced the graphs for NGC 288, we used parameters that reproduced the values that Grillmair *et al.* found for the central density, the tidal radius, and the core radius ($\sigma_0 = 4217$ stars/(armin^2), $r_t = 15.6$

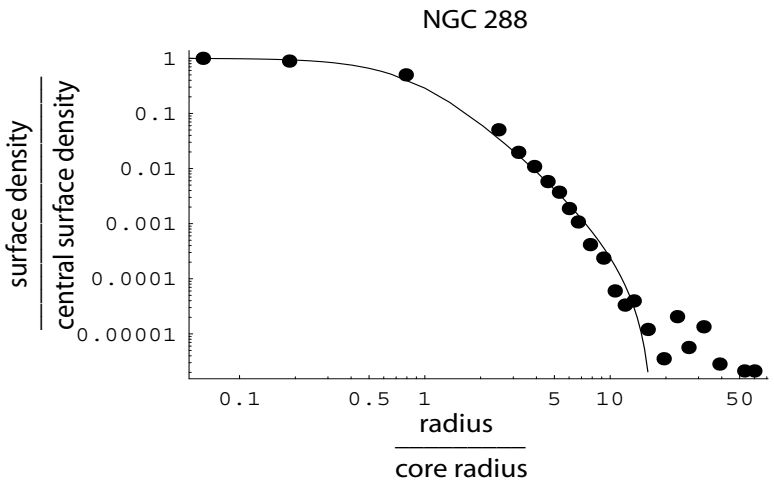

Figure 8: σ/σ_0 vs. R ($R_t = 17$, $R_a = 1$)

arcmin, $r_c = 0.06$ arcmin). We again varied the two parameters (R_t and R_a) until we got a result we were satisfied with. Figure 9 is the resulting Michie model fitted to NGC 5824 with $R_t = 260$, and $R_a = 1$ - still using the Grillmair *et al.* values for the core radius. Notice that the shape of the Michie model resembles the shape of the data, but the position of the curve is off. A probable explanation for this is that the chosen core radius and the fitted central density for NGC 5824 are too low. Readjusting these values ($r_c = 0.24$ arcmin, and $\sigma_0 = 14125$ stars/(armin^2)), we get a much more accurate fit (see Figure 10). It is important to remark that had we changed the King model to these new values for R_c and σ_0, it would still be a bad fit because the shape of the King distribution would not change, it would simply be shifted to the right and upward. Again, it is interesting to notice that the Michie model that fits the data the best has a very anisotropic velocity dispersion.

Up to this point, Grillmair *et al.'s* explanation for the discrepancy between the star counts and the King model has been that these tidal tails of stars are indeed no longer tidally bound to the cluster and are escaping, but they are doing so at a very slow rate. However, our Michie model fits suggest that perhaps these tidal stars *are* still bound to the cluster and that the tidal radius is larger than first calculated. Also,

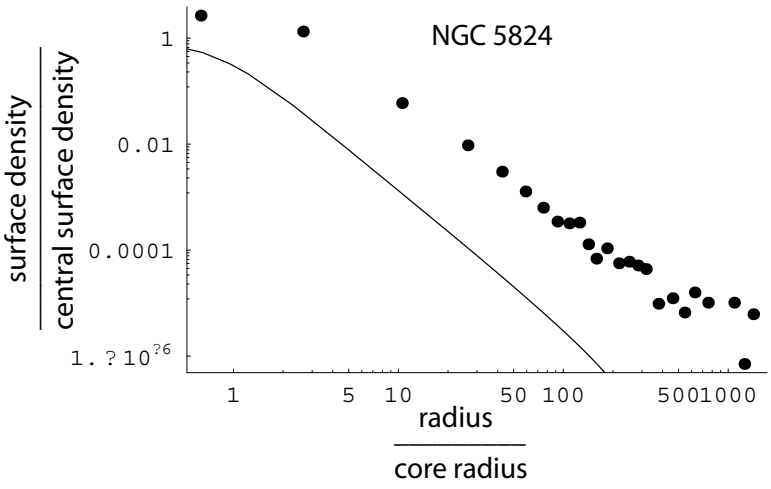

Figure 9: σ/σ_0 vs. R ($R_t = 260$, $R_a = 1$)

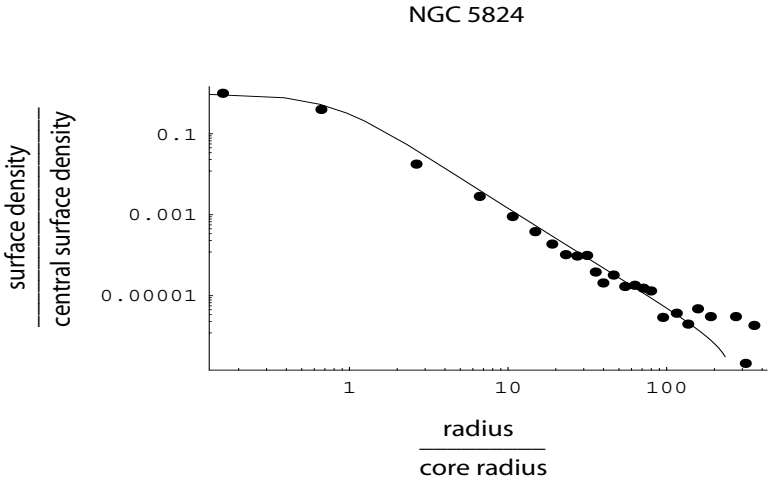

Figure 10: $\sigma/\sigma 0$ vs. R ($R_t = 260$, $R_a = 1$, $r_c = 0.24$, $\sigma_0 = 14125$)

the fact that the Michie model fits the clusters better than a King model re-enforces the belief that globular clusters have a very anisotropic velocity dispersion.

5 Two-component Model

An interesting study done by Roueff, Salati, and Taillet showed that if a certain amount of (low mass) dark matter was introduced into the Michie model, the velocity dispersion and surface brightness profile paralleled that of the King model. In other words, a two component anisotropic model (with properly chosen parameters) can be made indistinguishable from a one component isotropic model [3].

This result was somewhat anticipated because it is known that dark matter flattens the velocity dispersion, while in the presence of anisotropy the velocity dispersion becomes less flat. The two effects cancel each other out and thus Michies model with dark matter appears to be identical to a one component isotropic model. Moreover, even though dark matter is present in the two component model, we cannot distinguish it from a one component model; thus, we cannot trace dark matter through velocity dispersions or surface brightness profiles. In the following section, we attempt that trace the presence of dark matter through surface density profiles.

5.1 Michie Model with Second Mass

To add dark matter to the Michie model, we must first re-examine Eq. (19). A more convenient way to express this model is to define $H(W, \alpha)$ as follows:

$$H(W, \alpha) = e^W \int_0^W d\eta (e^{-\eta} - e^{-W}) \eta^{\frac{1}{2}} \int_0^1 dy \; e^{-\alpha^2 \eta (1-y^2)}, \tag{21}$$

where $\alpha = r/r_a$. Thus, the one component model is simply $H(W, \alpha)$ up to a scaling factor. Now we can introduce dark matter by defining the dimensionless mass $M = m_2/m_1$, where m_1 is the visible mass and m_2 is the dark matter mass. Depending on our choice of j, m_1 is set to 1 in the one component Michie model. However, since the

potential is the same for the dark matter component, we can write the distribution function for the second component as:

$$f_2(r,v) = k_2 e^{-Mj^2L^2/r_{a2}^2}\left(e^{2Mj^2\epsilon}-1\right)\theta(-2V(r)-v^2), \tag{22}$$

where r_{a2} allows for a different anisotropy radius than the visible r_a. If we now define $\eta = Mj^2v^2$, $W = -2j^2V(r)$, $\alpha_2 = r/r_{a2}$, and $y = \cos\theta$,

$$f_2(r,v) = k_2 e^{-{\alpha_2}^2\eta(1-y^2)}\left(e^{MW-\eta}-1\right)\theta(MW-\eta). \tag{23}$$

Since $\rho_2(r) = m_2 \int d^3v\ f_2(r,v)$,

$$\rho_2(r) = 2\pi m_2 k_2 M^{-3/2} j^{-3} e^{MW}\int_0^{MW} d\eta (e^{-\eta}-e^{-MW})\eta^{\frac{1}{2}}\int_0^1 dy\ e^{-{\alpha_2}^2\eta(1-y^2)}. \tag{24}$$

Using our $H(W,\alpha)$ notation, Eq. (24) becomes:

$$\rho_2(r) = 2\pi k_2 m_2 M^{-3/2} j^{-3} H(MW,\alpha_2) \tag{25}$$

To simplify things even further, we can replace k_1 in ρ_1 with its central density ρ_{c1} and k_2 in ρ_2 with ρ_{c2} (note that before we were calling the central density ρ_0). Thus,

$$\rho_1(r) = \rho_{c1}\frac{H(W,\alpha_1)}{H(W_0,0)}, \tag{26}$$

and

$$\rho_2(r) = \rho_{c2}\frac{H(MW,\alpha_2)}{H(MW_0,0)} \tag{27}$$

Once again, we now have ρ_1 and ρ_2 in terms of W (or in our case in terms of $H(W,\alpha)$), but what we wish is to have ρ_1 and ρ_2 together in terms of R (where again $R = r/r_c$). Rewriting Poisson's equation ${\nabla_r}^2 V(r) = 4\pi G\rho(r)$ yields:

$${\nabla_R}^2 W(R) = -8\pi j^2 {r_c}^2(\rho_1+\rho_2), \tag{28}$$

where $\rho(r) = \rho_1 + \rho_2$ and $8\pi j^2 {r_c}^2 G\rho_{c1} = 9$ as before. Therefore, the complete differential equation becomes:

$${\nabla_R}^2 W(R) = -9\frac{\rho_1+\rho_2}{\rho_{c1}} = -9\left(\frac{H(W,\alpha_1)}{H(W_0,0)} + \frac{\rho_{c2}}{\rho_{c1}}\frac{H(MW,\alpha_2)}{H(MW_0,0)}\right). \tag{29}$$

Just as before, we use Mathematica to solve this differential equation, and project our final $\rho(R)$ onto the sky to get $\sigma(R)$ by the technique developed earlier (see King model).

5.2 Two-Component Model Results

As we had done earlier in this paper with the King and Michie model, we fit our two-component model to the star count data of two globular clusters (NGC 288 and NGC 5824). In this two-component model there are considerably more parameters one can vary, namely: M, r_{a1}, r_{a2}, ρ_{c2}/ρ_{c1}, and r_t. In our fits, we set $M = .1$, $r_{a1} = r_{a2} = 1$, r_t to be the same as in the best Michie model result, and varied ρ_{c2}/ρ_{c1}. Our rational for these choices was the following: since we are considering only low mass dark matter objects in this paper, we set one dark matter object(like a planet) to be 1/10 of the mass of a visible matter object(star); hence, $M = 0.1$. From our results with the Michie model, it is apparent that globular clusters have a very anisotropic velocity dispersion, thus we set r_{a1}=$r_{a2} = 1$. Next the parameter ρ_{c2}/ρ_{c1} tells us the numerical ratio of dark to light matter objects. Since $M = .1$, if $\rho_{c2}/\rho_{c1} = 1$, we know that the total dark to light matter ratio by total mass is 1/10, whereas if $\rho_{c2}/\rho_{c1} = 10$, then there is a 1:1 dark to light matter ratio by total mass.

The first fit we made on NGC 288 (fig.(11)) was with $\rho_{c2}/\rho_{c1} = 1$ and a readjusted $r_c = 3.2$ arcmin. This figure is a slightly better fit than the Michie model (fig.(4)), but there is still relatively very little dark matter (1:10 dark to light matter ratio by total mass). The next fit on NGC 288 (fig.(12)) was with $\rho_{c2}/\rho_{c1} = 10$ (1:1 dark to light matter ratio by total mass), and already, this fit is poor regardless of how you readjust r_c.

We next fit the two-component model to NGC 5824, see fig.(13). However, as seen from this plot, even with $\rho_{c2}/\rho_{c1} = 1$, the fit is poor, implying that for $\rho_{c2}/\rho_{c1} = 10$, the fit would be even worse. Adding more matter to the globular cluster is pulling

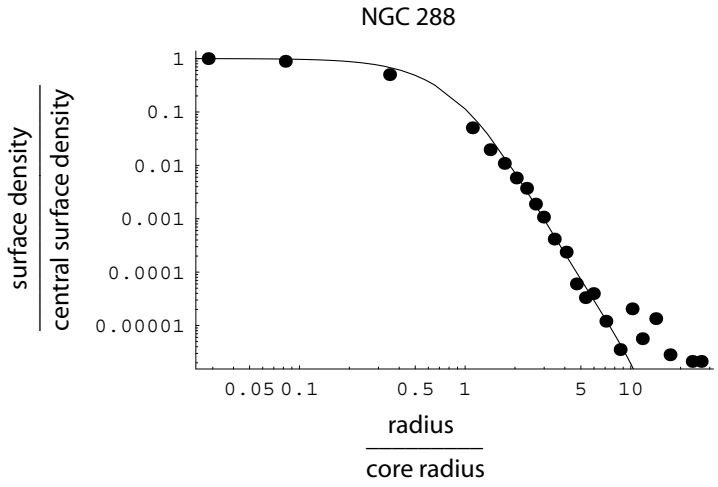

Figure 11: $\sigma/\sigma 0$ vs. R ($R_t = 17$, $R_{a1} = R_{a2} = 1$, $M = .1$, $\rho_{c2}/\rho_{c1} = 1$, $r_c = 3.2$)

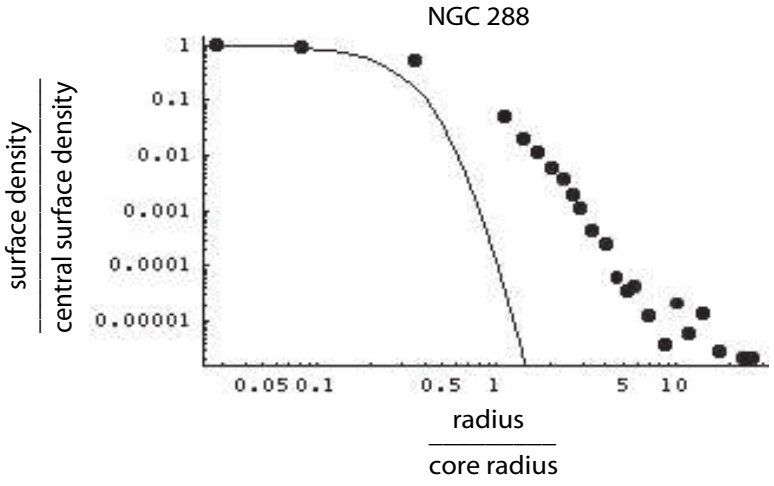

Figure 12: $\sigma/\sigma 0$ vs. R ($R_t = 17$, $R_{a1} = R_{a2} = 1$, $M = .1$, $\rho_{c2}/\rho_{c1} = 10$, $r_c = 3.2$)

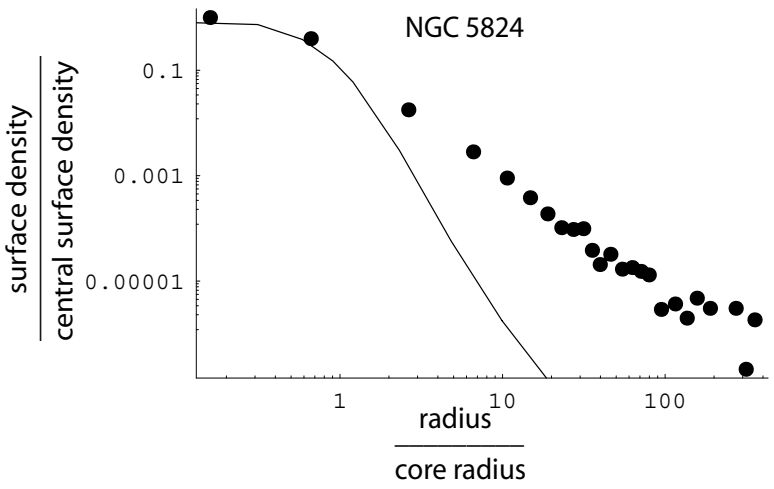

Figure 13: $\sigma/\sigma 0$ vs. R ($R_t = 260$, $R_{a1} = R_{a2} = 1$, $M = .1$, $\rho_{c2}/\rho_{c1} = 1$, $r_c = 3.2$)

everything closer together, making the fit fall off too fast to match our observed data. In other words, in NGC 5824 our model implies that there is less than a 1:10 dark to light matter ratio by total mass. The fits for NGC 288 and NGC 5824 implicate that there are few, if any, dark matter objects in these globular clusters. However, there is a serious limitation to consider in our two-component model. According to the model, nothing can exist beyond r_t, so there is no way of testing a case in which the dark matter halo extends to infinity, or even beyond the visible matter. Although there may be dark matter distributed throughout all of space, our model only allows the radius of the dark matter halo to be less than or equal to r_t. Therefore, we conclude that looking at the surface density profile with the two-component Michie model will give inconclusive results to the amount of dark matter in a globular cluster.

6 Conclusions and Future Research

In this thesis, we fit King and Michie surface density distribution functions to Grillmair *et al.'s* data to two globular clusters. A major result is that the fits considerably improved when the radius of anisotropy in the Michie model is small. This implies

that globular clusters have very anisotropic velocity dispersions; in different words, stellar orbits in these globular clusters are quite eccentric. Despite the predisposition by many authors to use the King model, the Michie model is more appropriate to fit these stellar structures.

An area of future research is to continue working with this two-component model to see how much dark matter can be put in without affecting the fit of the Michie model (despite the limitation to the model discussed in the previous section). This type of research would give a bound on the amount of dark matter that can exist in a globular cluster. Preliminary work reported here suggests that there is little, if any, dark matter enbedded in the globular clusters we have examined. Yet another research topic to pursue is to see how changing gravity affects the star count distribution, and whether it will solve the discrepancies between the theoretical distribution model and the observed star count data.

References

[1] Shu, F.H., The Physical Universe: An Introduction to Astronomy. University Science Books, 1982.

[2] Hayli, A. Dynamics of Stellar Systems. Spitzer, L.Jr, Dynamical Theory of Spherical Stellar Systems with Large N. I.A.U., 1975.

[3] Roueff, F., Salati, P., Taillet, R. 1997, AJ.

[4] www.relativity.livingreviews.org

[5] Grillmair *et al.*, C.J., Freeman, K.C., Irwin, M., and Quinn, P.J. 1995, AJ 109, 2553.

[6] Moore, B., 1996, ApJ 461, L13.

[7] Oh, K.S., and Lin, D.N.C. 1992, ApJ 386, 519.

[8] King, I.R., 1965, AJ 70, 376.

[9] King, I.R., 1966, AJ 71, 64.

[10] Michie, R.W., 1963 MNRAS 126, 499.

[11] Michie, R.W., 1961, ApJ 133, 781.